

# STABILIZATION FOR HAPTIC INTERFACE DEVICE IN NETWORKED VIRTUAL REALITY ENVIRONMENT

Khaing Zar Win

UCSY-Ishibashi Lab., Faculty of Computer Science, University of Computer Studies, Yangon  
Yangon, Myanmar  
khaingzarwin@ucsy.edu.mm  
<https://www.ucsy.edu.mm>

Yutaka Ishibashi

Department of Business Management, Faculty of Business Administration, Aichi Sangyo University  
Okazaki, Aichi, 444-0005, Japan  
ishibasi@asu.ac.jp  
<https://www.asu.ac.jp>

Amy Tun

Faculty of Computer Systems and Technologies, University of Computer Studies, Yangon  
Yangon, Myanmar  
amytun@ucsy.edu.mm  
<https://www.ucsy.edu.mm>

Khaing Htet Win

Faculty of Computer Systems and Technologies, University of Computer Studies, PaThein  
PaThein, Myanmar  
khainghtetwin86@gmail.com

## Abstract

**This paper investigates the stabilization of a haptic interface device in a networked maze system, focusing on objective assessment using different performance metrics, such as local lag and moving velocity. Participants interact with a virtual environment where they are tasked with raising and moving a cube from a starting position to a target point in our experiment. The raising and moving method is applied in an experimental setup to enhance the stabilization of the device. Additionally, this paper examines the impact of different damper values on the device's stability, particularly when subjected to different moving velocities. The damper values are adjusted to mitigate unstable phenomena that can arise during device operation. The experiment results indicate that both moving velocity and local lag strongly correlate with the force feedback of the haptic interface device. Thus, we illustrate that changes in the variables significantly influence force feedback behavior, which is crucial for maintaining the device's stability and performance.**

**Keywords:** Stabilization; Raising method, Networked maze system, Haptic interface device; Force feedback; Networked virtual reality environment.

## 1. Introduction

A haptic interface device is a hardware tool that allows users to engage with virtual environments through tactile sensations. It delivers force feedback, or haptic feedback, by simulating touch-based sensations or forces to enrich the user's interaction. Haptic communication, which relies on the sense of touch, plays a crucial role in human interaction. In networked virtual environments, incorporating haptic feedback introduces an additional layer to the user experience, making interactions more immersive and lifelike [Huang (2013)].

Currently, many researchers are investigating various fields by incorporating haptic interface devices. These devices are utilized in a wide range of areas, such as education, art, aerospace, machinery, the military, artificial intelligence, big data, data science and analytics, robotics, virtual reality environments, real-time gaming, networked communication, multimedia communication, and more. Among these, networked gaming has become a particularly popular focus, as highlighted in this study through the use of haptic interface devices. When combining the Internet with haptic interface devices, force feedback becomes a crucial element in networked

virtual reality environments that involve haptic sensations. Factors such as network delay, jitter, and packet loss can significantly degrade Quality of Service (QoS), which in turn affects the assessment of Quality of Experience (QoE). Therefore, both QoS management and QoE evaluation are essential, as they are closely connected and influence each other.

Quality of Service (QoS) control and Quality of Experience (QoE) assessment are crucial for ensuring a satisfying and immersive haptic communication experience. QoS focuses on the technical aspects of delivering haptic feedback, such as managing network latency and reliability [Aung (2020)]. QoE, on the other hand, evaluates how users perceive and enjoy the overall experience [Win (2021)].

In haptic communication, there is a direct cause-and-effect relationship between QoS control and QoE assessment. Effective QoS control impacts the technical quality of haptic feedback, which in turn influences the user's perceived QoE. By optimizing technical factors like network delay, jitter, and packet loss, QoS control aims to enhance the overall user experience. Regular QoE assessments provide feedback that helps refine QoS measures, ensuring continuous improvement in the quality of the haptic experience.

When haptic communication is conducted over the Internet, issues such as network delay, jitter, and packet loss can significantly degrade QoE. Therefore, implementing robust QoS control measures is essential to minimize these issues and achieve the best possible QoE for users.

The stability of the haptic interface device is a crucial factor in achieving precise and accurate assessment results, reflecting its overall effectiveness [Wen (2019)]. In a networked virtual reality environment, the vibration of the haptic device influences the moving velocity and local lag, which can impact the quality of the user experience. Stabilization control in haptic communication is about ensuring that the feedback users receive through touch remains smooth and reliable, even when there are delays or disruptions in the network [Huang (2017)]. It involves using various techniques to adjust and correct the tactile sensations so that users experience consistent and accurate interactions with virtual environments. This control is crucial for maintaining a realistic and immersive experience, preventing issues like jitter or lag from affecting how users perceive and interact with virtual objects.

Reaction force control in haptic communication focuses on adjusting the forces transmitted back to users through a haptic device as they interact with virtual environments. This control aims to simulate realistic touch sensations, enhancing the user's immersion and engagement. Local lag, or the delay between a user's action and the resulting haptic feedback, is a key factor in this process [Oo (2022)]. Minimizing local lag is essential for ensuring that the feedback feels immediate and responsive [Win (2024)]. Additionally, the relationship between the user-controlled object's movement speed and the reaction force they experience is crucial. By accurately simulating how touch sensations vary with movement speed, the haptic system creates a more authentic and immersive experience, making interactions with virtual objects feel more realistic [Oo (2020)].

Applying damper values in a spring-damper model for networked haptic communication helps manage the stability of a haptic device as the moving speed increases. In this model, the damper controls how quickly the system absorbs and dissipates energy, which affects the device's response to user interactions. As the moving speed of the device increases, the risk of instability and erratic feedback also rises. By adjusting the damper value, you can fine-tune the system to handle higher speeds more effectively, reducing issues like jitter and maintaining smoother, more stable haptic feedback [Komatsu (2017)]. This adjustment is crucial for ensuring that the device remains responsive and reliable, even as users interact with the virtual environment at faster speeds.

The subsequent sections of this paper are organized as follows: Section II describes the networked maze system that incorporates haptic feedback. Section III explores Stabilization control and QoS control within haptic communication, discussing its significance and implications. Section IV details the methodology used in the experiments, focusing on the approach taken with the networked maze system and haptic feedback. Section V presents and analyzes the experimental results, examining performance metrics and the effects of variables such as local lag and moving velocity. Section VI summarizes the key findings and insights from the study, while Section VII concludes with the study's overall conclusions and recommendations for future research and development in the field.

## 2. Networked Maze System with Haptic

In the networked setup, a personal computer (PC) is connected to a haptic interface device via a network, functioning within a client/server framework as illustrated in Fig. 1. The objective in this setup is to manipulate a virtual box (referred to as a cube) from its initial position to a specified target location. This task is carried out using designated evaluation techniques and adhering to a predefined route.

In the virtual environment, the acceleration due to gravity is set to zero, meaning the effects of gravity are not simulated. The dimensions of the virtual space are 20 cm in width, 15 cm in height, and 15 cm in depth. The virtual box within this space is 1 cm in size. These virtual dimensions are mapped to the physical workspace of the haptic interface device, which has a width of 16 cm, a height of 12 cm, and a depth of 7 cm. This mapping allows users to interact with the virtual environment through the haptic interface device, which provides force feedback and tactile sensations that correspond to the virtual objects within these specified dimensions.

## 2.1. Configuration setting

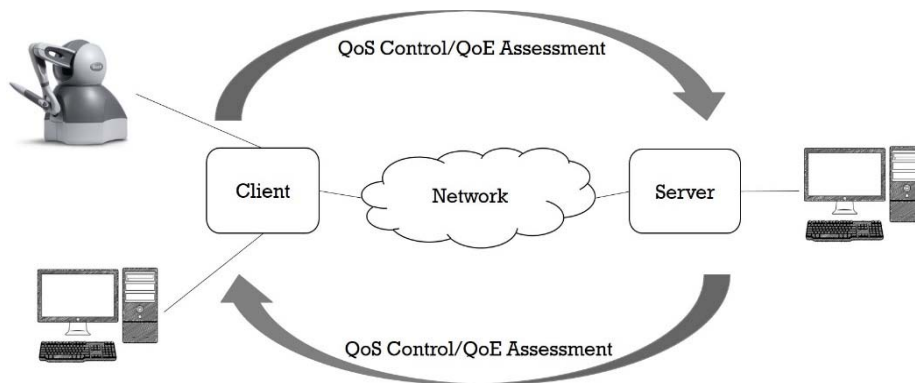


Fig. 1. Configuration setting of networked communication system with haptic.

In the configuration of the haptic communication setup shown in Fig. 1, two PCs and one haptic interface device are used. Both PCs are connected to the Internet, with one PC linked to the haptic interface device. In this setup, one PC acts as the client, while the other functions as the server. The process utilizes the raising method, where the cursor is positioned at the bottom of the cube to guide the object from its starting position to the target point.

In the networked virtual environment shown in Fig. 2, the initial setup involves setting the local lag to its default value, which places the box at a predetermined starting position. During the experiment, the raising method is used to control the movement of the box. The cursor is placed at the bottom of the box to guide it along a predefined path from the starting point to the target position within the networked maze system, which includes walls, partitions, a starting position, a target point, and a small circle representing the cursor. The goal is to navigate the virtual box to the target location using the raising method. If the box collides with walls or partitions, or if there is a disconnect between the box and the cursor, the process will pause. It resumes from the point of disconnection once the cursor is repositioned, or it may terminate and restart if necessary.

## 2.2. Calculation method

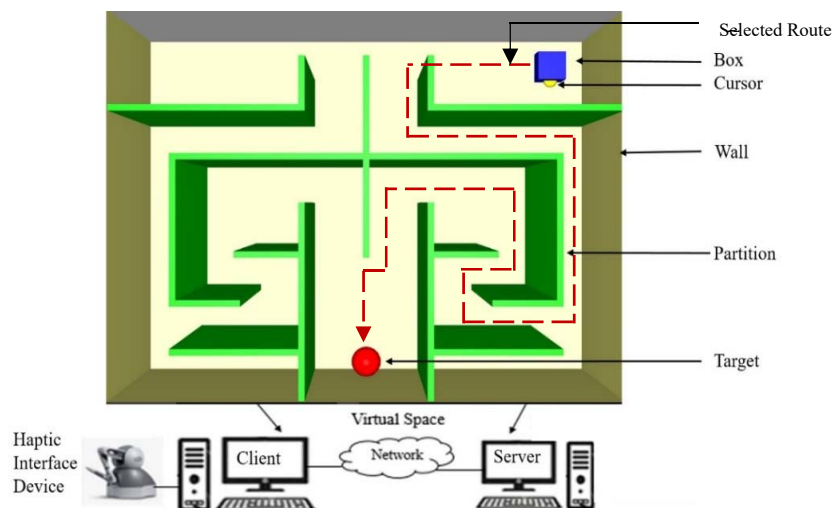


Fig. 2. Virtual reality environment of networked maze system in haptic communication.

In this study, the authors employed a calculation method for reaction force based on the user's movement and the interaction of force feedback. They considered moving speed in relation to distance, working time, and process operation time. This method allows for the precise assessment of how reaction forces are affected by the user's actions within the system.

### 2.2.1. Calculation method of Reaction force

Force feedback is crucial for delivering tactile sensations or force responses during interactions within a virtual environment, involving the generation of reaction forces by the haptic device. These forces simulate the feeling of interacting with virtual objects or environments. Elasticity, in this context, refers to the force exerted by springs, similar to the resistance felt when manipulating a spring. Viscosity describes the resistance encountered when moving objects through fluids like water or oil. In our experiment, the calculation method for reaction force is as follows:

$$F = -K_s Dh - K_d (V_c - V_b) \quad (1)$$

As described in Eq. (1), the reaction force  $F$  is calculated using the spring-damper model, where:  $F$  is the reaction force generated by the haptic device.  $K_s$  represents the elasticity (spring) coefficient, indicating the force exerted by the spring-like component.  $K_d$  is the viscosity (damper) coefficient, representing the resistance due to damping.  $Dh$  is a vector representing the movement of the cursor from the starting position to its current position.  $V_c$  is the velocity of the cursor.  $V_b$  is the velocity of the box. This equation captures the combined effects of elasticity and viscosity to simulate realistic force feedback in the haptic system.

The reaction force is calculated not only when raising the virtual box from the cursor via the stylus tip of the haptic interface device but also during collisions, such as when the box impacts a wall or partition. For these collision scenarios, we use an alternative calculation method to determine the reaction force. This method is outlined as follows:

$$F = -K_s x - K_d v \quad (2)$$

In Eq. (2), the reaction force  $F$  is determined using the following parameters:  $F$  is the reaction force.  $K_s$  represents the coefficient of elasticity (spring) value.  $K_d$  denotes the coefficient of viscosity (damper) value.  $x$  is the penetration depth, which measures how deeply the virtual box penetrates into the wall or partition upon collision.  $v$  is the relative velocity between the cursor and the object. This equation calculates the reaction force based on both the depth of penetration and the relative velocity during collisions, incorporating elasticity and viscosity effects.

### 2.2.2. Calculation method of Moving velocity

The moving velocity is defined as the distance traveled from the starting point to the target position divided by the time taken to cover this distance. The calculation for moving velocity is given by the following equation:

$$V = D/T \quad (3)$$

According to Eq. (3),  $V$  represents the moving velocity of the cursor,  $D$  is the distance traveled, and  $T$  is the time taken to travel from the starting position to the end point. In the experiment conducted, ten different moving velocity values were tested, ranging from 0.3 to 3.0 with intervals of 0.3. This range of velocities was used to obtain precise and accurate results in the study.

### 2.2.3. Calculation method of Operation time

The time spent traveling from the starting point to the end position is referred to as the operation time. The operation time  $T_{opt}$  is calculated using the following Eq. (4).

$$T_{opt} = E_{opt} - S_{opt} \quad (4)$$

In here,  $T_{opt}$  is the operation time,  $E_{opt}$  is the end of operation time and  $S_{opt}$  is the starting time of operation.

## 3. Stabilization Control and QoS Control in Haptic Communication

Stabilization control in a haptic interface device refers to the mechanisms used to maintain the stability and position of the device while providing haptic feedback to the user. In order to provide accurate and precise haptic feedback, the device must be able to maintain a stable position and resist external forces that may cause it to move or vibrate. This is particularly important in applications where the user is manipulating objects or interacting with a virtual environment, as even small movements or vibrations can disrupt the experience and reduce the effectiveness of the haptic feedback. These mechanisms may be passive, such as springs or dampers, or active, to actively counteract external forces.

Quality of Service (QoS) control in haptic communication is essential for providing a smooth and realistic user experience. This involves managing the transmission of tactile feedback in virtual environments to ensure low latency, high reliability, and consistency. In this paper, the authors focus on the reaction force and local lag within a networked maze system of haptic communication, highlighting how these factors impact the overall effectiveness and realism of the haptic feedback.

Quality of Service (QoS) control in haptic communication is key to managing various parameters that ensure realistic and timely force feedback. Force feedback, or haptic feedback, involves generating forces, vibrations, or motions in response to user interactions within a virtual environment or simulation. The aim is to recreate the sensations of real-world interactions, thereby enhancing user immersion. Reaction force control is a critical component within this framework, as it directly affects the quality of the user's experience by influencing how accurately and effectively the virtual environment responds to user actions.

Reaction force control in haptic communication involves managing and simulating the forces that users experience when interacting with haptic devices or virtual environments. This aspect of haptic communication, which focuses on the sense of touch, aims to deliver a realistic and immersive experience by replicating tactile sensations. In haptic devices like force-feedback controllers or robotic systems, effective reaction force control is essential for creating a convincing and interactive user experience, enhancing how users perceive and interact with the virtual world.

Reaction force control specifically involves the precise adjustment of forces that the haptic device exerts on the user's hand. This control enables the simulation of various tactile sensations, such as resistance, texture, or interactions with virtual objects. It is particularly important in applications like virtual reality (VR) and teleoperation systems, where users engage with virtual or remote environments. In gaming, reaction force control enhances the experience by providing realistic feedback during interactions with virtual objects. Overall, this aspect of haptic communication is vital for creating a compelling and immersive user experience, allowing users to engage with virtual environments through authentic force feedback.

Local lag control involves buffering local data for a set period to address network delays in networked multimedia applications, especially in collaborative 3D virtual environments. This mechanism helps maintain consistency between user terminals by compensating for network latency. Data related to user actions or interactions, such as positional information and inputs, is stored temporarily at a user's terminal. This buffering ensures that despite the network delay, the interactions remain synchronized and consistent across all terminals in the collaborative virtual environment.

Local lag, which refers to the predetermined time period for buffering, is set according to the estimated or measured network delay between the local terminal and other terminals. This approach allows for accounting for variations in network latency. By implementing local lag control, each terminal introduces a delay in the local data to compensate for network delays. This strategy ensures a consistent and synchronized experience across all participating terminals, minimizing the risk of desynchronization or inconsistencies in the virtual environment.

In haptic communication, local lag refers to the delay between a user's input or action and the haptic feedback they receive. Minimizing this lag is essential for ensuring a responsive and realistic user experience. In this study, the authors examined local lag by starting from 0 ms and progressively increasing up to 10 ms to explore its effects on the haptic maze communication system. The goal was to understand how various levels of latency impact user interactions and experiences. To evaluate the reaction force across different local lags, ten moving velocities were tested, ranging from 0.3 to 3.0 in intervals of 0.3, providing precise and accurate results for the experiments.

#### 4. Assessment Method

As detailed in this paper, the raising and moving method involves placing the cursor at the base of a virtual box and maneuvering the object from its starting position to a specified target location along a set path. When the system starts, the virtual box appears at the pre-established starting position. The raising and movement method is utilized within the networked maze system that incorporates haptic feedback, following a predefined route as illustrated in Fig. 2, as part of the experimental methodology.

This study explores how variations in the damper ( $K_d$ ) value and local lag affect the stability of a haptic interface device in a networked maze system for each moving speed. Initially, both the local lag and  $K_d$  values are set to zero. The local lag is then gradually increased in 10 ms intervals until vibrations are detected. At that point, the  $K_d$  value is incremented by 0.1 to stabilize the system. This process continues, with further adjustments to the local lag, until the system becomes unstable again. This study highlights that the  $K_d$  value plays a crucial role in mitigating vibrations in the haptic interface device, although the distances at which vibrations occur vary.

In this paper, we highlight the process of determining and estimating the optimum values for  $K_d$  and  $K_s$  in the context of force feedback in a haptic interface device, based on moving velocity and local lag. By plotting both the actual optimum values and the estimated values from the regression equations, we can visually confirm the goodness of fit. It's particularly interesting to note that the optimum  $K_d$  value results in higher local lag and lower reaction force compared to the  $K_s$  values in relation to local lag and force feedback for each moving speed. We observe that the optimum  $K_d$  value with local lag is greater than the  $K_s$  value with local lag, where optimum value of  $K_d$  is greater than the value of  $K_s$ . In here, we defined the value of  $K_s$  is the second largest local lag value in each moving speed. This suggests that as local lag increases, the optimum  $K_d$  value tends to result in a higher reaction force compared to  $K_s$ . If the local lag is equal for both optimum  $K_d$  and  $K_s$ , the reaction force is not the same; specifically, the reaction force for optimum value with  $K_d$  is less than the force feedback for the value of  $K_s$ .

By applying ten different moving velocities, the study likely explores how the interaction between the damper values and the speed of movement affects stability. Higher velocities might introduce greater instability, requiring more effective damping. The goal of this examination is to find the optimal damper values that can maintain stability across all tested velocities, ensuring consistent and reliable haptic feedback regardless of how fast the user is moving the device.

The working process incorporates a checkpoint mechanism: if the box detaches from the cursor, the process stops immediately. To resume, the cursor is repositioned at the base of the box, allowing the task to continue until it is completed.

The process continuously monitors for collisions between the object and walls or partitions. When a collision occurs, the operation pauses until the cursor is accurately aligned at the bottom of the box. Once properly aligned, the process resumes. If the cursor is not correctly positioned, the process is terminated and restarted to ensure proper execution. This approach ensures accuracy and maintains the integrity of the task, requiring precise alignment for seamless progress.

The experiment is replicated ten times for each combination of local lag and movement velocity. The authors then calculated the average operation time and the average of the average reaction force across varying movement speeds and different local lag values, employing multiple regression analysis to interpret the results.

In this study, we explore the impact of various damper values on the stability of a haptic interface device, especially when exposed to ten different moving velocities. These damper values are adjusted to address and mitigate any instability that may arise during the use of the device. Damping is a technique used to reduce oscillations or vibrations within a system. In haptic devices, adjusting the damper values can help control the feedback the user receives, making the interaction smoother and more stable. Instability in a haptic interface might manifest as jittery or erratic feedback, making it difficult for the user to control the device accurately. This can be especially problematic when the device is used in a networked environment where latency or other delays are present.

This study highlights the critical factors in the networked maze system with haptic communication. The relationship between force strength, local lag, moving velocity, and the  $K_d$  (damper) value is central to the system's stability and operability. As both local lag and moving speed increase, so does the reaction force, which is crucial for maintaining the haptic interface device's performance. The  $K_d$  value, by absorbing vibrations, plays a significant role in ensuring a stable and effective interaction within the haptic environment. This demonstrates the importance of carefully controlling these variables to achieve the desired haptic feedback and system stability.

## 5. Assessment Results

This paper investigates how variations in the damper ( $K_d$ ) value and local lag impact the stability of a haptic interface device in a networked maze system for each moving velocity. Initially, both the local lag and  $K_d$  values are set to zero. The local lag is then incrementally increased by 10 ms until vibrations are observed. At this point, the  $K_d$  value is raised by 0.1 to stabilize the system. This process continues, with further increases in local lag, until the system becomes unstable again. The study underscores the critical role of the  $K_d$  value in reducing vibrations in the haptic interface device, although the distances at which vibrations occur vary.

In the networked maze system using the raising and moving method, the experimental results are illustrated from Fig. 3 to Fig. 12. These figures show that the optimal  $K_d$  (damper) value, as well as the distances of local lags, vary depending on the moving velocity.

In Fig. 3, the assessment results display the average reaction force versus local lag, with various symbols indicating different  $K_d$  (damper) values and their corresponding optimum  $K_d$  values, all based on a moving velocity of 0.3. In Fig. 3, the damper value ( $K_d=0$ ) reaches 30 ms, ( $K_d=0.1$ ) reaches 40 ms, and ( $K_d=0.2$ ) reaches 70 ms. Therefore, the optimum  $K_d$  is determined to be 0.2, as it corresponds to the longest local lag distance in a moving velocity of 0.3, in this paper. This figure demonstrates that both the distance of local lag and the reaction force vary depending on the  $K_d$  value. From this figure, the optimum  $K_d$  value can be identified as the one associated with the longest local lag and lowest force feedback.

Similarly, Fig. 4 illustrates the average reaction force versus local lag, with different symbols representing various  $K_d$  (damper) values and their corresponding optimum  $K_d$  values, at a moving velocity of 0.6. The figure shows that the distance of local lag and the reaction force differ depending on the  $K_d$  value. In this paper, the damper values yield the following local lag times:  $K_d=0$  reaches 20 ms,  $K_d=0.1$  reaches 20 ms,  $K_d=0.2$  reaches 30 ms, and  $K_d=0.3$  reaches 60 ms in Fig.4. Therefore, the optimum  $K_d$  is determined to be 0.3, as it corresponds to the longest local lag distance at a moving velocity of 0.6. From this figure, the optimum  $K_d$  value can also be determined as the one linked with the longest local lag and lowest reaction force.

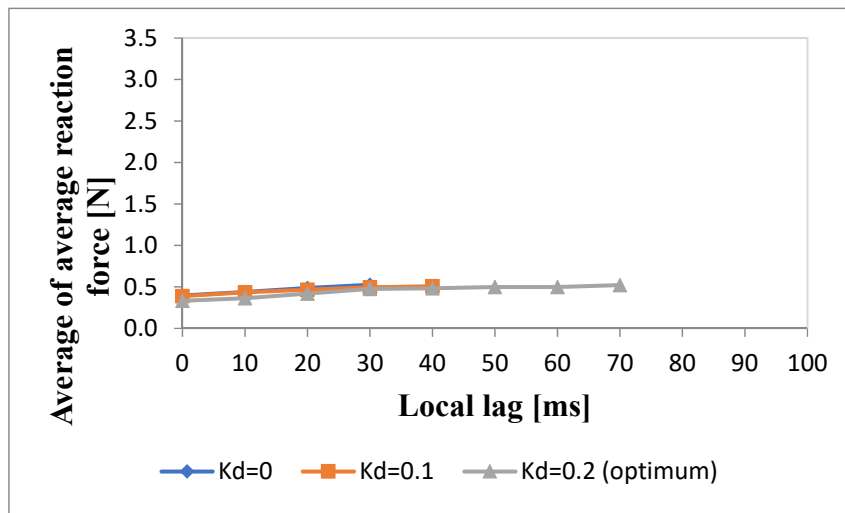


Fig. 3. Average of average reaction force versus local lag when moving velocity is 0.3.

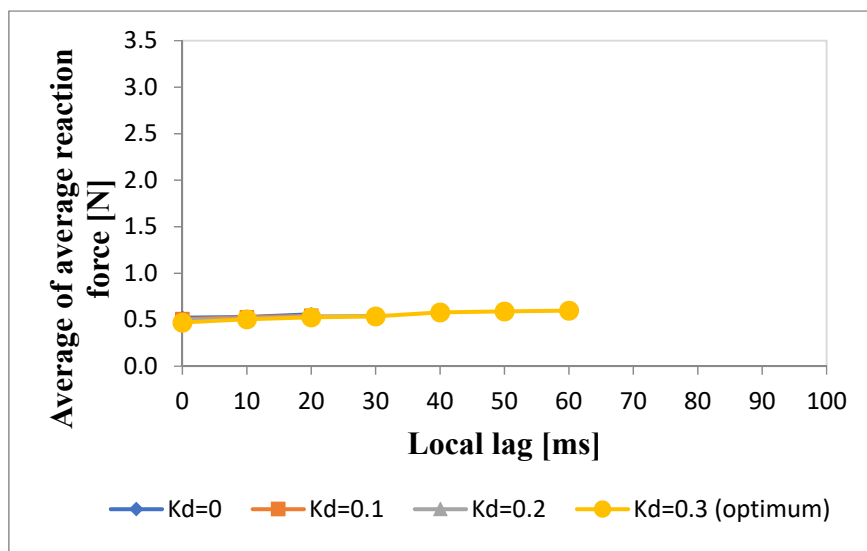


Fig. 4. Average of average reaction force versus local lag when moving velocity is 0.6.

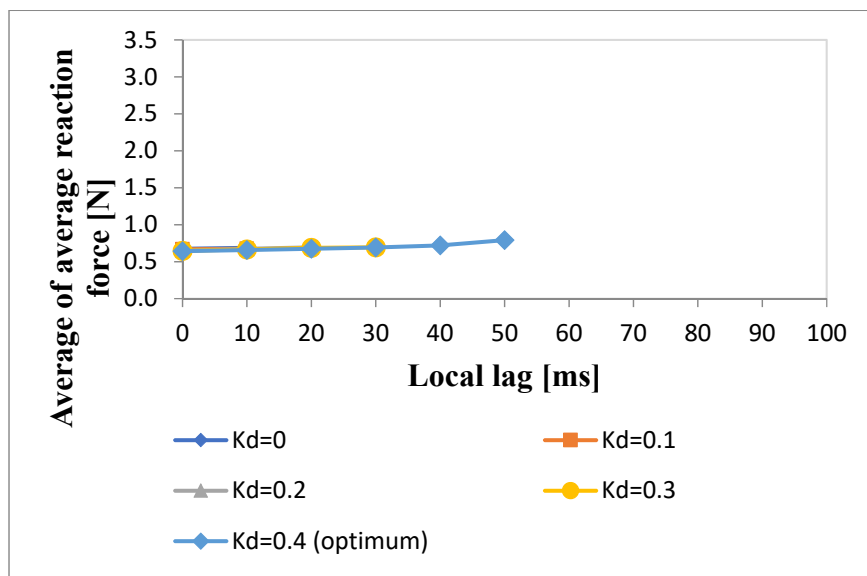


Fig. 5. Average of average reaction force versus local lag when moving velocity is 0.9.

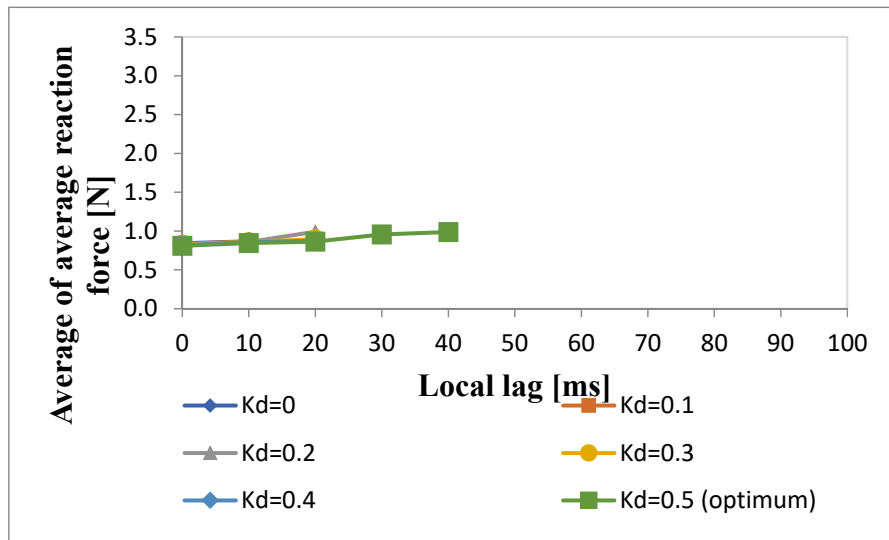


Fig. 6. Average of average reaction force versus local lag when moving velocity is 1.2.

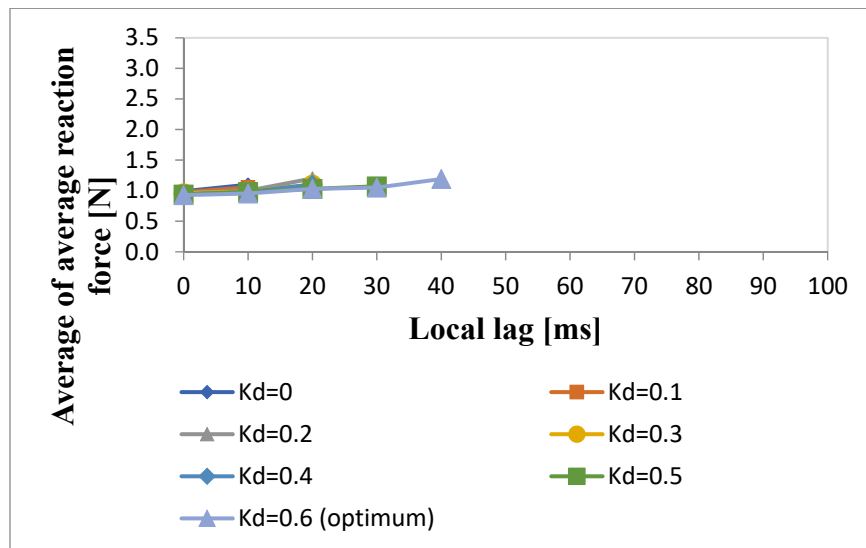


Fig. 7. Average of average reaction force versus local lag when moving velocity is 1.5.

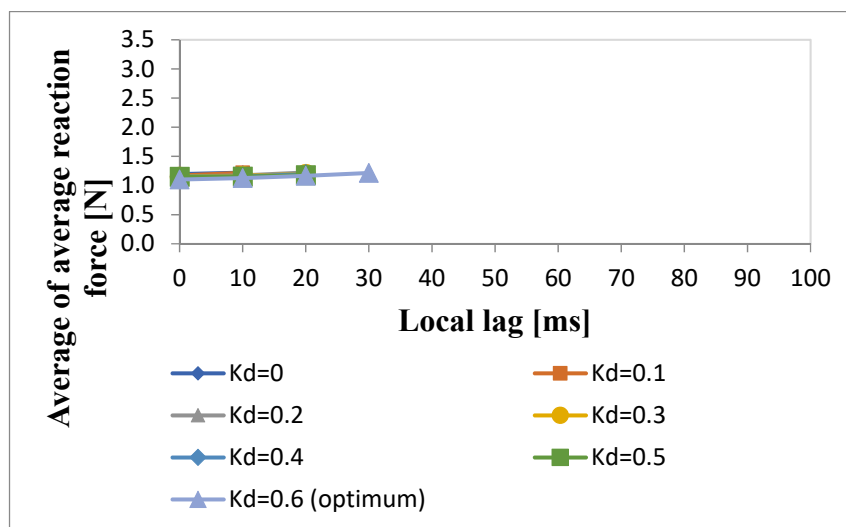


Fig. 8. Average of average reaction force versus local lag when moving velocity is 1.8.



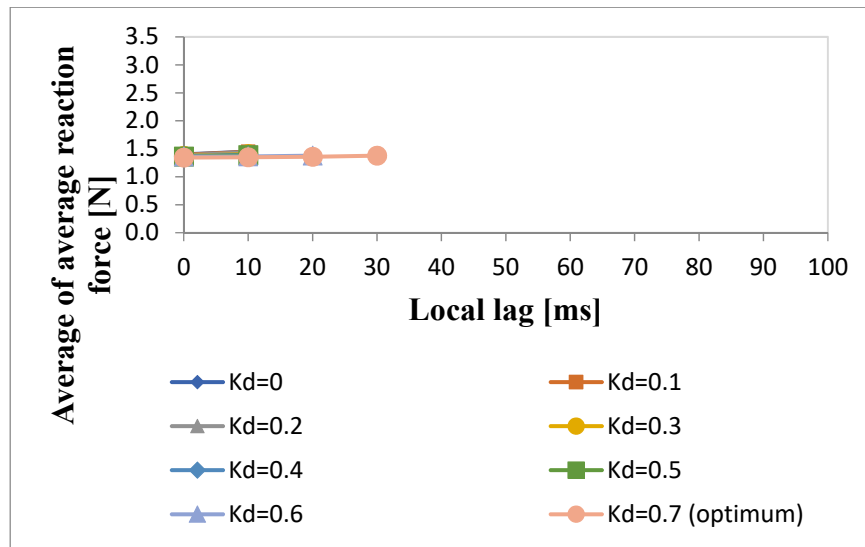


Fig. 9. Average of average reaction force versus local lag when moving velocity is 2.1.

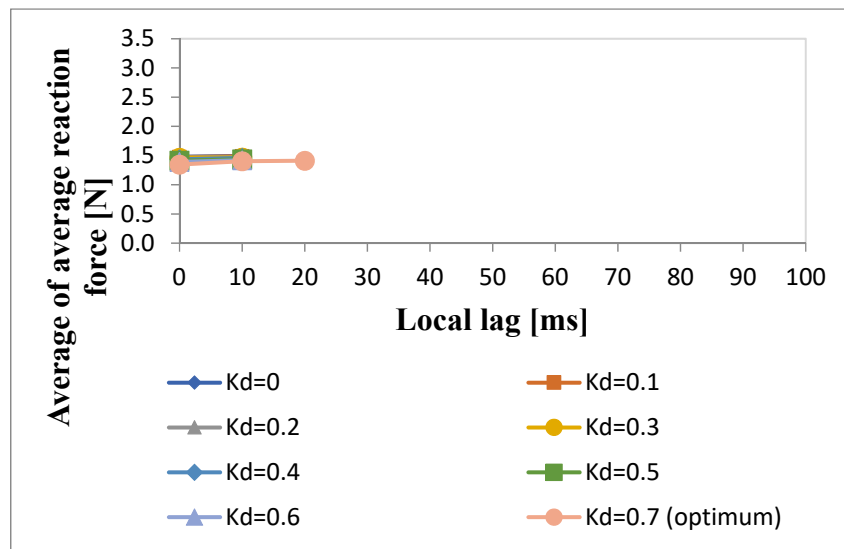


Fig. 10. Average of average reaction force versus local lag when moving velocity is 2.4.

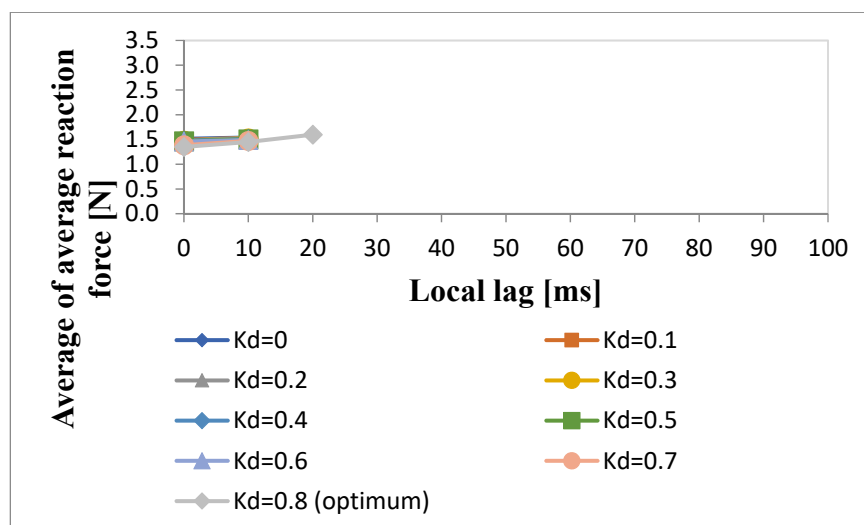


Fig. 11. Average of average reaction force versus local lag when moving velocity is 2.7.

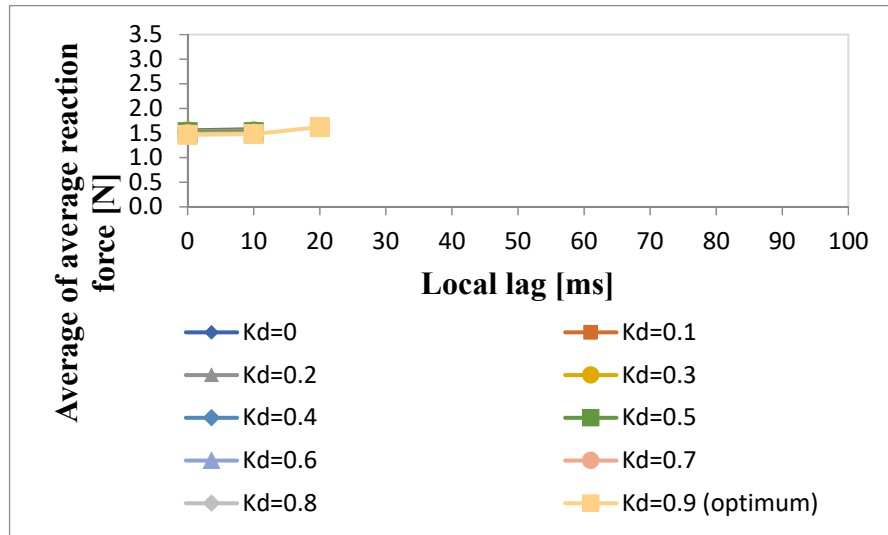


Fig. 12. Average of average reaction force versus local lag when moving velocity is 3.0.

From Fig. 5 through Fig. 12, which illustrate the average reaction force versus local lag, different symbols represent various Kd (damper) values and their corresponding optimum Kd values at moving velocities ranging from 0.9 to 3.0, with an interval of 0.3. These figures collectively show that the distance of local lag and the reaction force vary depending on the Kd value for each moving speed. The optimum Kd value is identified as the one associated with the longest local lag in each case. Additionally, as moving speed increases, both the Kd and optimum Kd values tend to be larger to handle the stability of haptic interface device, while the distance of local lags becomes shorter.

The optimum values of Kd and Ks are determined from figures that show the average of average force versus the local lag and moving velocity for various values of Kd. Therefore, these optimum values do not have corresponding regression equations. On the other hand, the estimated optimum values of Kd and Ks are obtained through regression analysis, which provides regression equations with a coefficient of determination ( $R^2$ ) that indicates the goodness of fit between the regression equation and the actual optimum values. The regression analysis results show that the optimum Kd value is given by  $2.435 \times 10^{-2} L_l + 2.886 \times 10^{-1} M_v$ , with a determination coefficient ( $R^2$ ) of 0.9959, and the Ks value is given by  $1.925 \times 10^{-3} L_l + 2.588 \times 10^{-1} M_v$ , with an  $R^2$  of 0.9964. The regression analysis results for the relationship equations of the optimum Kd and the value of Ks is  $1.36 \times 10^{-3} L_l + 9.26 \times 10^{-3} M_v + 1.07 K_s$  and, the contribution determination ( $R^2$ ) is 0.9999. In this context, the equations can be expressed using the local lag ( $L_l$ ) and the moving velocity ( $M_v$ ). The optimum values of Kd and Ks can be determined based on  $L_l$  and  $M_v$ . These equations can be obtained through multiple regression analysis. This indicates a strong correlation between the optimum Kd and Ks values with moving velocity and local lag, respectively.

Table 1 presents the results of the multiple regression analysis conducted with ten different moving velocities. In the table,  $F$  represents the reaction force and  $L_l$  denotes the local lag. The determination coefficient,  $R^2$ , exceeds 0.81, indicating a strong relationship between local lag, reaction force, and the Kd (damper) values and its optimum Kd value. This high  $R^2$  value suggests that the local lag and reaction force are significantly influenced by the Kd value and its corresponding optimum value, depending on the moving speed. In Table 1, which details the local lag values depending on the damper value (Kd) and the optimum Kd value, it is noted that the maximum local lag value reached varies for each moving velocity and is not the same across all velocities. Thus, precise and accurate equations for force feedback can be derived for each moving speed, reflecting the robust connection between these variables.

| Moving velocity | Local lag (ms) | Kd               | Equations   | $R^2$  |
|-----------------|----------------|------------------|---|--------|
| 0.3             | 30             | Kd=0             | $F=4.4 \times 10^{-3} L_l + 3.973 \times 10^{-1}$ | 0.9985 |
|                 | 40             | Kd=0.1           | $F=3.0 \times 10^{-3} L_l + 3.993 \times 10^{-1}$ | 0.9643 |
|                 | 70             | Kd=0.2 (optimum) | $F=2.7 \times 10^{-3} L_l + 3.559 \times 10^{-1}$ | 0.8841 |
| 0.6             | 20             | Kd=0             | $F=1.8 \times 10^{-3} L_l + 5.191 \times 10^{-1}$ | 0.8918 |
|                 | 20             | Kd=0.1           | $F=1.8 \times 10^{-3} L_l + 5.076 \times 10^{-1}$ | 0.9970 |
|                 | 30             | Kd=0.2           | $F=1.5 \times 10^{-3} L_l + 4.994 \times 10^{-1}$ | 0.9362 |
|                 | 60             | Kd=0.3 (optimum) | $F=2.2 \times 10^{-3} L_l + 4.786 \times 10^{-1}$ | 0.9641 |
| 0.9             | 10             | Kd=0             | $F=1.3 \times 10^{-3} L_l + 6.746 \times 10^{-1}$ | 1.0000 |
|                 | 10             | Kd=0.1           | $F=7.0 \times 10^{-4} L_l + 6.682 \times 10^{-1}$ | 1.0000 |
|                 | 20             | Kd=0.2           | $F=2.2 \times 10^{-3} L_l + 6.500 \times 10^{-1}$ | 0.9972 |
|                 | 30             | Kd=0.3           | $F=1.7 \times 10^{-3} L_l + 6.484 \times 10^{-1}$ | 0.9618 |

|     |    |                  |  |        |
|-----|----|------------------|--|--------|
|     | 50 | Kd=0.4 (optimum) | $F=2.7 \times 10^{-3}L+6.285 \times 10^{-1}$ | 0.8882 |
| 1.2 | 10 | Kd=0             | $F=2.3 \times 10^{-3}L+8.437 \times 10^{-1}$ | 1.0000 |
|     | 10 | Kd=0.1           | $F=3.1 \times 10^{-3}L+8.349 \times 10^{-1}$ | 1.0000 |
|     | 20 | Kd=0.2           | $F=8.1 \times 10^{-3}L+8.122 \times 10^{-1}$ | 0.8863 |
|     | 20 | Kd=0.3           | $F=3.4 \times 10^{-3}L+8.255 \times 10^{-1}$ | 0.9997 |
|     | 30 | Kd=0.4           | $F=3.0 \times 10^{-3}L+8.196 \times 10^{-1}$ | 0.9540 |
|     | 40 | Kd=0.5 (optimum) | $F=4.6 \times 10^{-3}L+7.995 \times 10^{-1}$ | 0.9445 |
| 1.5 | 10 | Kd=0             | $F=1.1 \times 10^{-2}L+9.893 \times 10^{-1}$ | 1.0000 |
|     | 10 | Kd=0.1           | $F=8.1 \times 10^{-3}L+9.752 \times 10^{-1}$ | 1.0000 |
|     | 20 | Kd=0.2           | $F=1.2 \times 10^{-2}L+9.366 \times 10^{-1}$ | 0.8561 |
|     | 20 | Kd=0.3           | $F=7.0 \times 10^{-3}L+9.450 \times 10^{-1}$ | 0.8819 |
|     | 20 | Kd=0.4           | $F=8.0 \times 10^{-3}L+9.269 \times 10^{-1}$ | 0.9211 |
|     | 30 | Kd=0.5           | $F=4.5 \times 10^{-3}L+9.372 \times 10^{-1}$ | 0.9976 |
| 1.8 | 40 | Kd=0.6 (optimum) | $F=6.2 \times 10^{-3}L+9.065 \times 10^{-1}$ | 0.9133 |
|     | 10 | Kd=0             | $F=2.5 \times 10^{-3}L+1.195 \times 10^0$    | 1.0000 |
|     | 10 | Kd=0.1           | $F=4.7 \times 10^{-3}L+1.171 \times 10^0$    | 1.0000 |
|     | 20 | Kd=0.2           | $F=3.4 \times 10^{-3}L+1.150 \times 10^0$    | 0.9323 |
|     | 20 | Kd=0.3           | $F=2.3 \times 10^{-3}L+1.149 \times 10^0$    | 0.9345 |
|     | 20 | Kd=0.4           | $F=2.4 \times 10^{-3}L+1.143 \times 10^0$    | 0.8373 |
| 2.1 | 20 | Kd=0.5           | $F=1.4 \times 10^{-3}L+1.145 \times 10^0$    | 0.8076 |
|     | 30 | Kd=0.6 (optimum) | $F=3.8 \times 10^{-3}L+1.098 \times 10^0$    | 0.9790 |
|     | 10 | Kd=0             | $F=5.1 \times 10^{-3}L+1.399 \times 10^0$    | 1.0000 |
|     | 10 | Kd=0.1           | $F=5.2 \times 10^{-3}L+1.395 \times 10^0$    | 1.0000 |
|     | 10 | Kd=0.2           | $F=5.4 \times 10^{-3}L+1.383 \times 10^0$    | 1.0000 |
|     | 10 | Kd=0.3           | $F=3.2 \times 10^{-3}L+1.374 \times 10^0$    | 1.0000 |
| 2.4 | 10 | Kd=0.4           | $F=2.6 \times 10^{-3}L+1.369 \times 10^0$    | 1.0000 |
|     | 10 | Kd=0.5           | $F=2.4 \times 10^{-3}L+1.360 \times 10^0$    | 1.0000 |
|     | 20 | Kd=0.6           | $F=9.0 \times 10^{-4}L+1.372 \times 10^0$    | 0.8788 |
|     | 30 | Kd=0.7 (optimum) | $F=1.1 \times 10^{-3}L+1.339 \times 10^0$    | 0.9261 |
|     | 10 | Kd=0             | $F=1.5 \times 10^{-3}L+1.479 \times 10^0$    | 1.0000 |
|     | 10 | Kd=0.1           | $F=1.5 \times 10^{-3}L+1.475 \times 10^0$    | 1.0000 |
| 2.7 | 10 | Kd=0.2           | $F=6.0 \times 10^{-4}L+1.468 \times 10^0$    | 1.0000 |
|     | 10 | Kd=0.3           | $F=4.0 \times 10^{-4}L+1.464 \times 10^0$    | 1.0000 |
|     | 10 | Kd=0.4           | $F=2.6 \times 10^{-3}L+1.436 \times 10^0$    | 1.0000 |
|     | 10 | Kd=0.5           | $F=2.2 \times 10^{-3}L+1.413 \times 10^0$    | 1.0000 |
|     | 10 | Kd=0.6           | $F=3.0 \times 10^{-3}L+1.392 \times 10^0$    | 1.0000 |
|     | 20 | Kd=0.7 (optimum) | $F=3.3 \times 10^{-3}L+1.355 \times 10^0$    | 0.8577 |
| 3.0 | 10 | Kd=0             | $F=2.3 \times 10^{-3}L+1.515 \times 10^0$    | 1.0000 |
|     | 10 | Kd=0.1           | $F=3.9 \times 10^{-3}L+1.495 \times 10^0$    | 1.0000 |
|     | 10 | Kd=0.2           | $F=5.3 \times 10^{-3}L+1.481 \times 10^0$    | 1.0000 |
|     | 10 | Kd=0.3           | $F=4.5 \times 10^{-3}L+1.479 \times 10^0$    | 1.0000 |
|     | 10 | Kd=0.4           | $F=3.7 \times 10^{-3}L+1.478 \times 10^0$    | 1.0000 |
|     | 10 | Kd=0.5           | $F=4.0 \times 10^{-3}L+1.464 \times 10^0$    | 1.0000 |
| 3.0 | 10 | Kd=0.6           | $F=3.2 \times 10^{-3}L+1.459 \times 10^0$    | 1.0000 |
|     | 10 | Kd=0.7           | $F=8.6 \times 10^{-3}L+1.386 \times 10^0$    | 1.0000 |
|     | 20 | Kd=0.8 (optimum) | $F=1.3 \times 10^{-2}L+1.341 \times 10^0$    | 0.9886 |
|     | 10 | Kd=0             | $F=2.3 \times 10^{-3}L+1.553 \times 10^0$    | 1.0000 |
|     | 10 | Kd=0.1           | $F=1.0 \times 10^{-3}L+1.546 \times 10^0$    | 1.0000 |
|     | 10 | Kd=0.2           | $F=5.0 \times 10^{-4}L+1.544 \times 10^0$    | 1.0000 |
| 3.0 | 10 | Kd=0.3           | $F=2.0 \times 10^{-4}L+1.538 \times 10^0$    | 1.0000 |
|     | 10 | Kd=0.4           | $F=2.0 \times 10^{-4}L+1.526 \times 10^0$    | 1.0000 |
|     | 10 | Kd=0.5           | $F=2.0 \times 10^{-5}L+1.519 \times 10^0$    | 1.0000 |
|     | 10 | Kd=0.6           | $F=7.0 \times 10^{-4}L+1.486 \times 10^0$    | 1.0000 |
|     | 10 | Kd=0.7           | $F=5.0 \times 10^{-4}L+1.482 \times 10^0$    | 1.0000 |
|     | 10 | Kd=0.8           | $F=3.0 \times 10^{-4}L+1.482 \times 10^0$    | 1.0000 |
|     | 20 | Kd=0.9 (optimum) | $F=8.0 \times 10^{-3}L+1.442 \times 10^0$    | 0.8195 |

Table 1. Optimum value of Kd for moving velocity and local lag.

Table 2 shows the optimum Kd values and their corresponding local lag and the value of Ks with its local lag according to each of moving velocity. In this table, the readers can see the local lag of optimum Kd and its values are greater than the local lag for Ks and its values.

| Moving velocity | Local lag for Kd (optimum) | Kd (optimum) | Local lag for Ks | Ks  |
|-----------------|----------------------------|--------------|------------------|-----|
| 0.3             | 70                         | 0.2          | 40               | 0.1 |
| 0.6             | 60                         | 0.3          | 30               | 0.2 |
| 0.9             | 50                         | 0.4          | 30               | 0.3 |

|     |    |     |    |     |
|-----|----|-----|----|-----|
| 1.2 | 40 | 0.5 | 30 | 0.4 |
| 1.5 | 40 | 0.6 | 30 | 0.5 |
| 1.8 | 30 | 0.6 | 20 | 0.5 |
| 2.1 | 30 | 0.7 | 20 | 0.6 |
| 2.4 | 20 | 0.7 | 10 | 0.6 |
| 2.7 | 20 | 0.8 | 10 | 0.7 |
| 3   | 20 | 0.9 | 10 | 0.8 |

Table 2. Optimum value of  $K_d$  and  $K_s$  for moving velocity and their corresponding local lag.

Fig. 13. through Fig. 22 presents the experiment results of the average of average reaction force versus local lag with different moving velocity that corresponding to the value of  $K_s$ . These figures demonstrate that when the moving velocity is greater, the force feedback is larger but local lag is less.

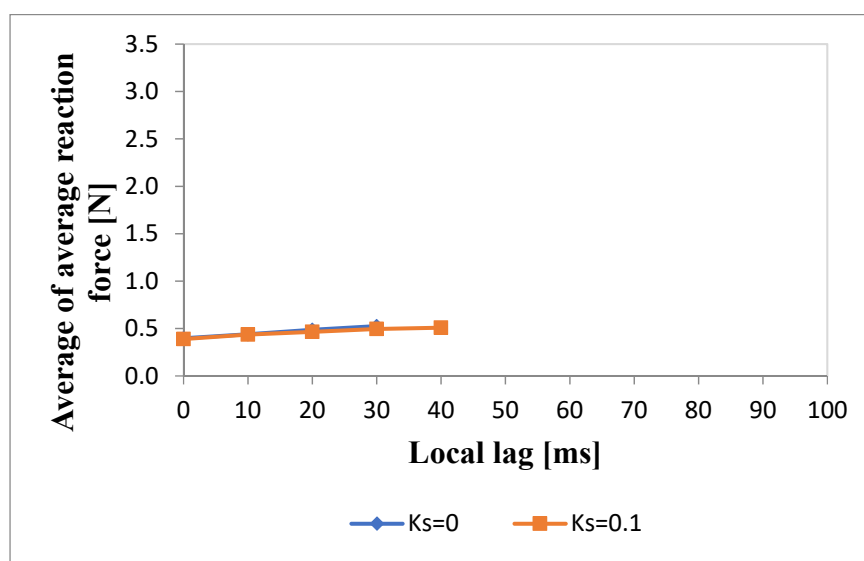


Fig. 13. Average of average reaction force versus local lag when moving velocity is 0.3.

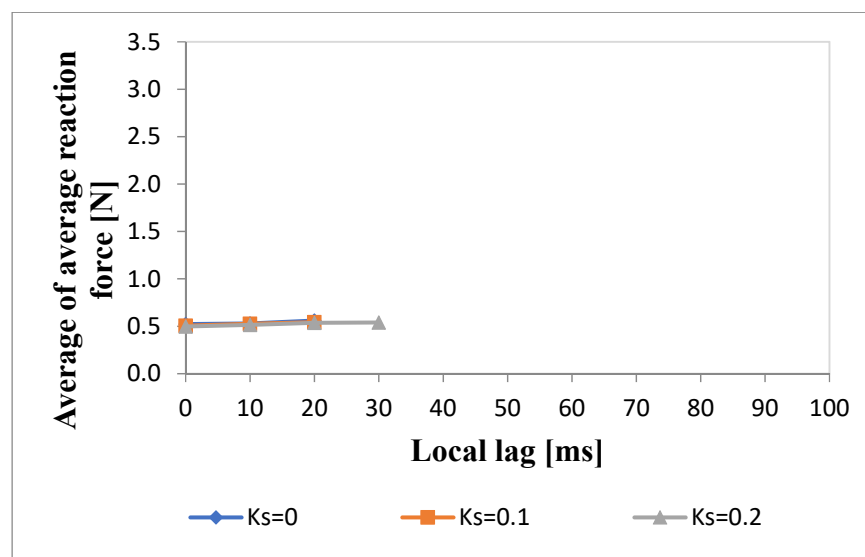


Fig. 14. Average of average reaction force versus local lag when moving velocity is 0.6.

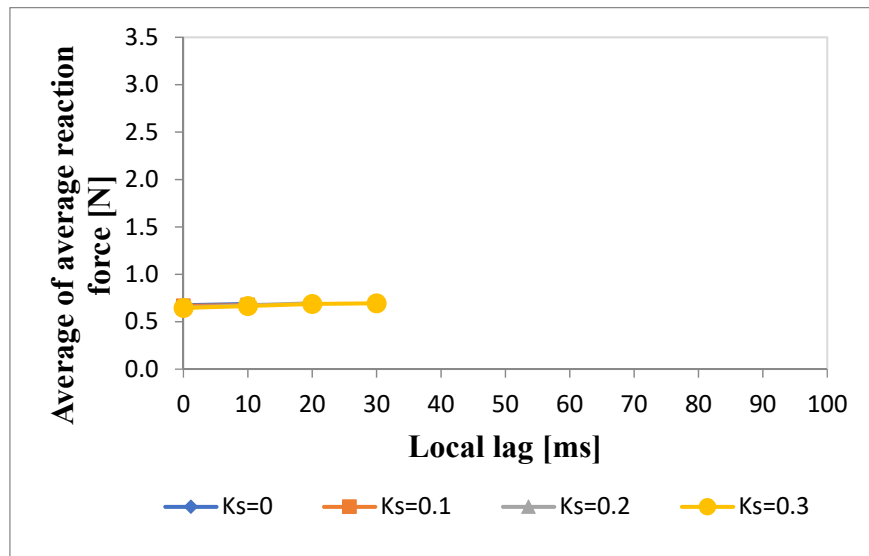


Fig. 15. Average of average reaction force versus local lag when moving velocity is 0.9.

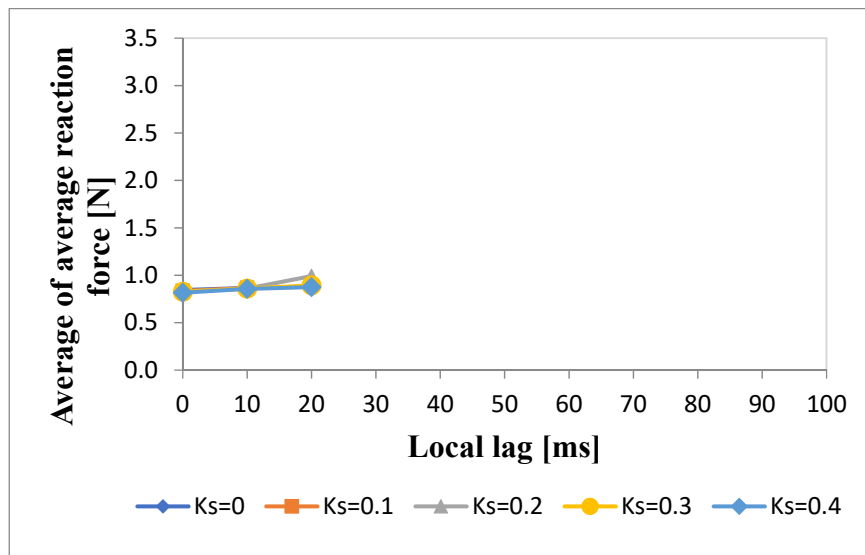


Fig. 16. Average of average reaction force versus local lag when moving velocity is 1.2.

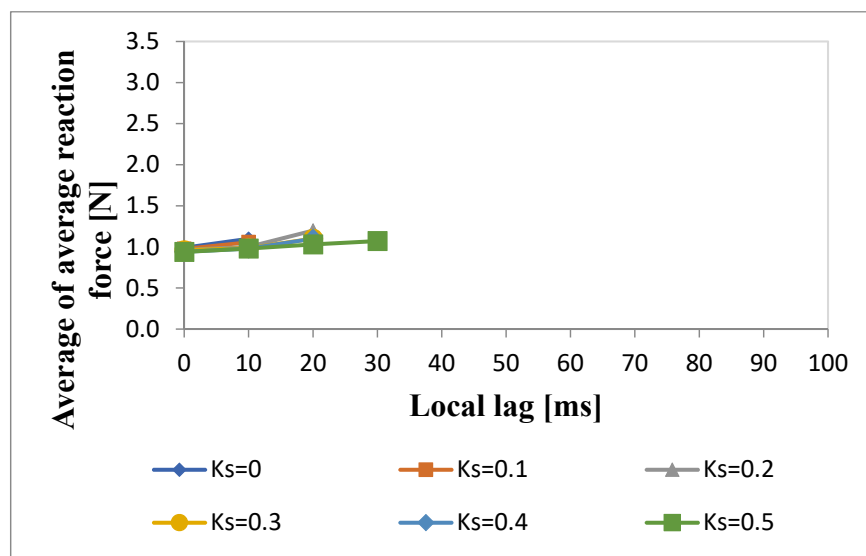


Fig. 17. Average of average reaction force versus local lag when moving velocity is 1.5.

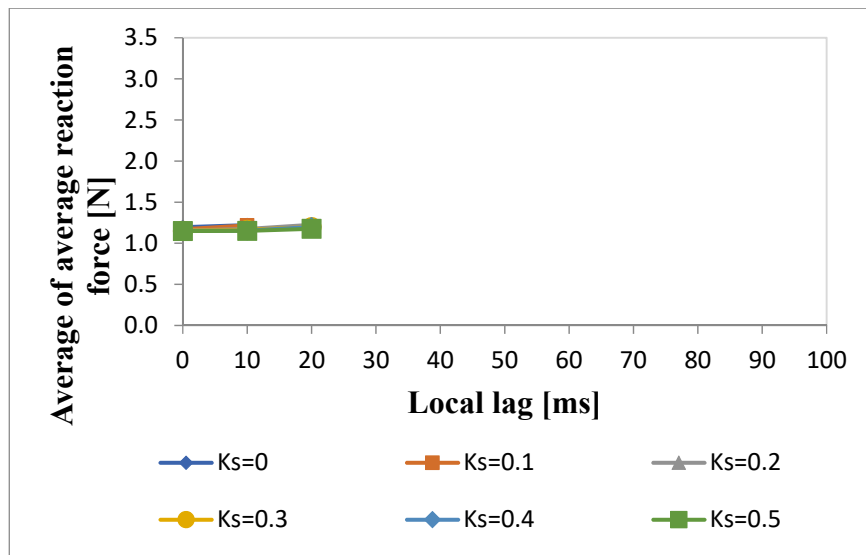


Fig. 18. Average of average reaction force versus local lag when moving velocity is 1.8.

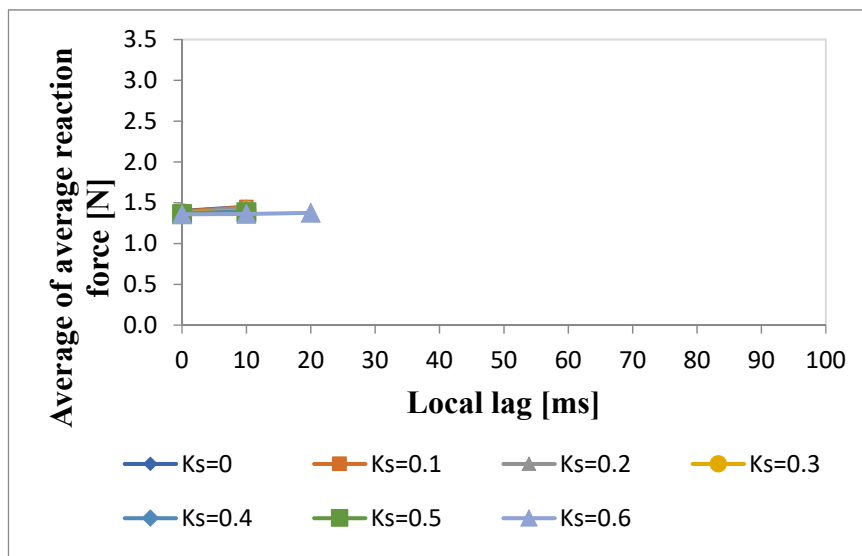


Fig. 19. Average of average reaction force versus local lag when moving velocity is 2.1.

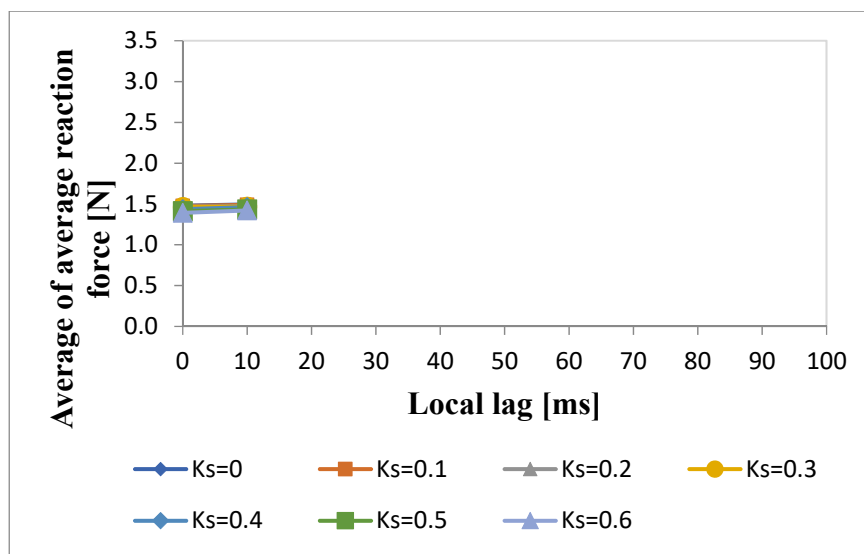


Fig. 20. Average of average reaction force versus local lag when moving velocity is 2.4.

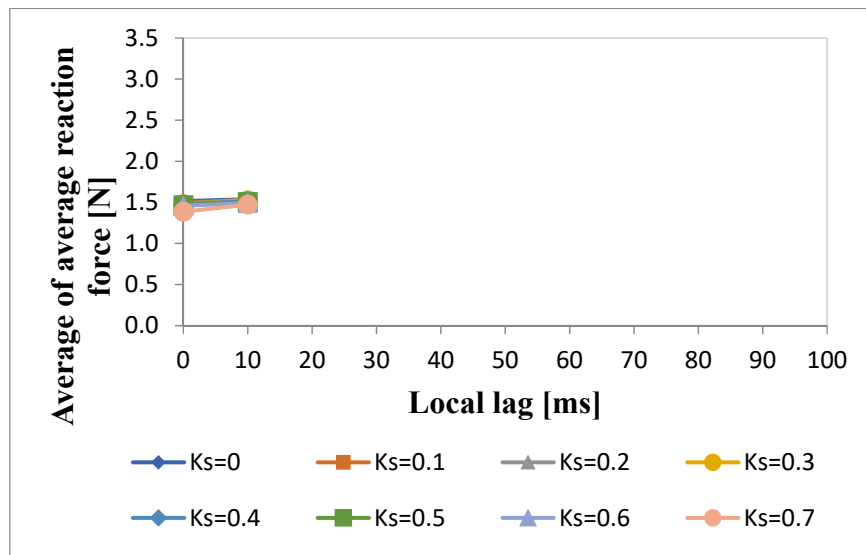


Fig. 21. Average of average reaction force versus local lag when moving velocity is 2.7.

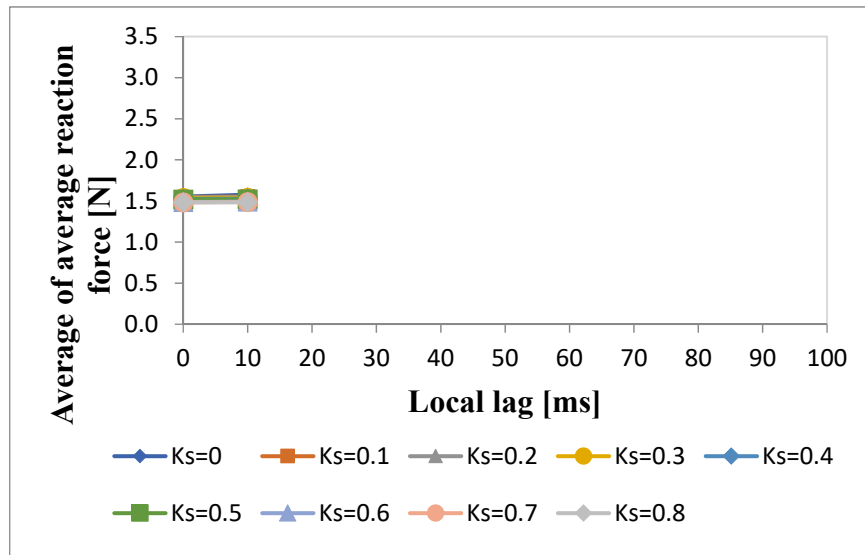


Fig. 22. Average of average reaction force versus local lag when moving velocity is 3.0.

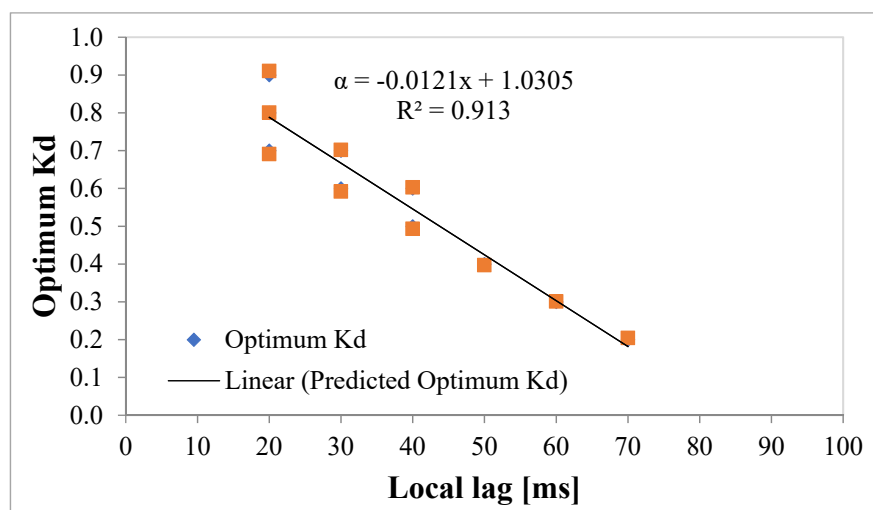


Fig. 23. Optimum Kd versus local lag.

Fig. 23 illustrates the relationship between the optimum Kd (damper) value and local lag. The symbols in the figure represent the experimentally determined optimum Kd values, while the line represents the predicted optimum Kd values obtained through regression analysis.

The purpose of this figure is to confirm the strong relationship between the optimum Kd and local lag. The close alignment of the symbols (experimental data) with the line (predicted values) would indicate that the regression model accurately predicts the optimum Kd values based on the local lag, thus validating the strong correlation between these variables.

The high coefficient of determination,  $R^2$  is 0.913, indicates that the regression model fits the data well, confirming that the optimum Kd is strongly correlated with the local lag. The satisfactory  $R^2$  value suggests that the model can reliably predict the optimum Kd for varying local lag values. This strong relationship is critical in fine-tuning the optimum Kd value for achieving stable performance in haptic interface devices, especially in the presence of varying local lag conditions.

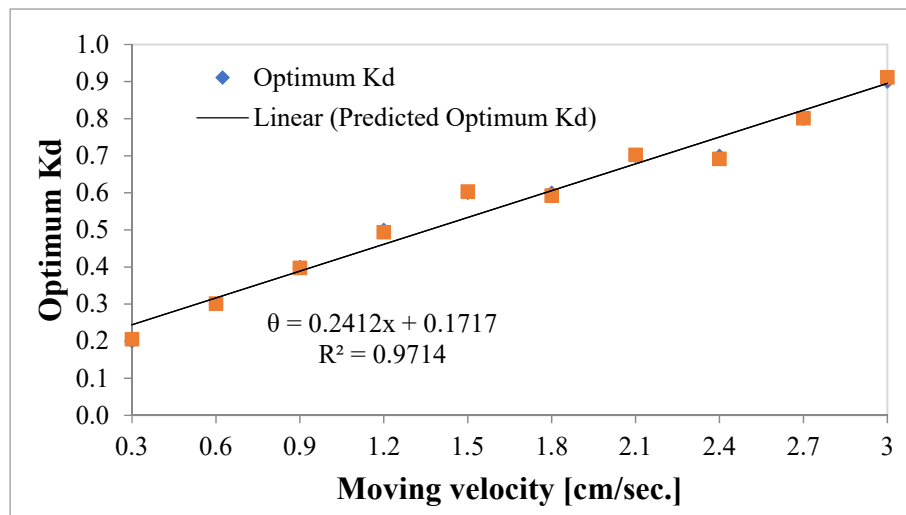


Fig. 24. Optimum Kd versus moving velocity.

In Fig. 24, the relationship between the optimum Kd (damper) value and moving velocity is depicted. The symbols in the figure represent the experimentally determined optimum Kd values, while the line represents the predicted optimum Kd values based on a regression model.

The alignment of the symbols (experimental data) with the line (predicted values) is used to confirm the strong relationship between the optimum Kd and moving velocity. If the symbols closely follow the line, it indicates that the regression model accurately predicts the optimum Kd values as a function of moving velocity, thereby validating the strong correlation between these variables.

The contribution determination ( $R^2$ ) value of 0.9714 further supports this strong relationship, indicating that the model explains approximately 97.14% of the variance in the optimum Kd values with respect to moving velocity. This high  $R^2$  value suggests that the model is highly satisfactory and reliable for predicting the optimum Kd based on moving velocity. This relationship is important because it suggests that the optimum Kd value can be effectively adjusted according to the moving velocity to maintain stability and performance in haptic interface devices.

In Figure 25, the relationship between the optimum Kd (damper) value and the Ks value is shown. The symbols in the figure represent the experimentally determined optimum Kd values, while the line represents the predicted optimum Kd values derived from a regression model.

The close alignment of the symbols (experimental data) with the line (predicted values) serves to confirm the strong relationship between the optimum Kd and Ks values. If the symbols closely follow the line, it indicates that the regression model is successful in predicting the optimum Kd values based on the corresponding Ks values, thereby validating the strong correlation between these two parameters. This strong correlation is further supported by the contribution determination result,  $R^2$  is 0.9992, indicating an almost perfect fit of the regression model to the data. This high  $R^2$  value confirms that the model is highly reliable in predicting the optimum Kd based on the Ks value.

This relationship is significant because it demonstrates that the optimum Kd value can be effectively predicted based on the Ks value. This interdependence is crucial for fine-tuning damping characteristics in haptic interface devices to achieve optimal stability and performance.



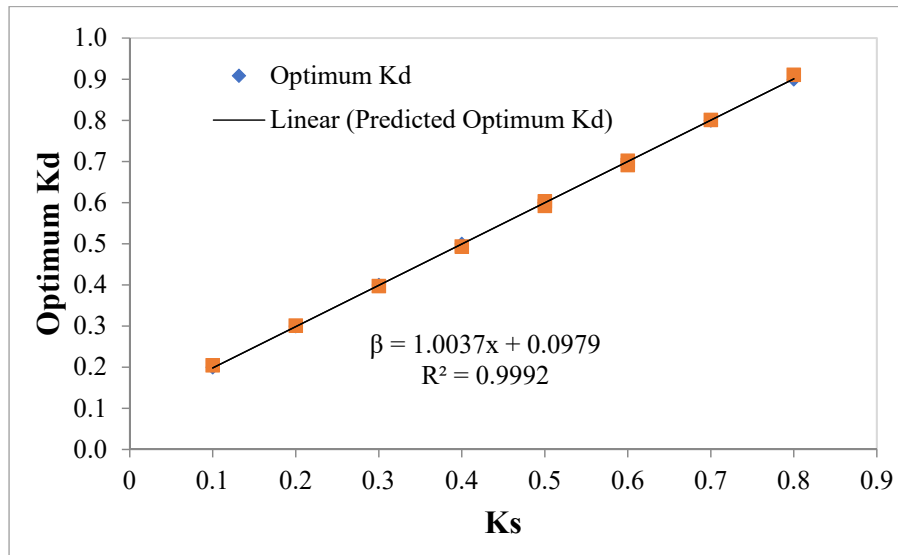


Fig. 25. Optimum Kd versus Ks.

## 6. Conclusion

This paper explores the stabilization of a haptic interface device within a networked maze system, focusing on various performance metrics such as local lag and moving velocity. Using the raising method in the experimental setup, this study aims to improve the stability of the haptic feedback by guiding participants to move a cube from a starting position to a target point along a predefined path. The raising method enhances the stability of the haptic feedback, ensuring smooth and consistent control despite challenges like local lag and moving speed. Additionally, this paper investigates how different damper values affect the device's stability across ten varying moving velocities, with the goal of mitigating instability during device operation.

We obtained the regression equations of optimum Kd and Ks values according to the moving velocity and local lag. Multiple regression analysis results show a strong correlation between Kd (damper) value, moving velocity, local lag, and the force feedback of the haptic interface device. This indicates that variations in these factors significantly affect the behavior of force feedback, which is essential for ensuring the device's stability and optimal performance.

## 7. Future Directions

By analyzing the Ks (spring) value, we will gain insight into how the spring component impacts the performance and stability of the haptic system, complementing our work with the Kd (damper) value. This approach will provide a more comprehensive understanding of how both damping and spring effects contribute to the overall haptic experience and system behavior.

Improving Quality of Service (QoS) control is indeed crucial for enhancing Quality of Experience (QoE) in haptic communication. Future efforts aim to expand QoE assessments to cover various networked environments, leveraging the findings from this study to refine and optimize haptic interactions across different settings. This approach will help ensure that users consistently experience high-quality and immersive haptic feedback, regardless of the specific network conditions or virtual environments.

## Acknowledgments

This study is the collaborative work of UCSY-Ishibashi Lab from the University of Computer Studies, Yangon, Myanmar and the Aichi Sangyo University, Aichi, 444-0005 Japan.

## Conflicts of Interest

The authors have no conflicts of interest to declare.

## References

- [1] Abe T and et. al., "QoE Assessment of Adaptive Viscoelasticity Control in Remote Control System with Haptic and Visual Senses", in Proc. 2018 IEEE International Conference on Consumer Electronics-Taiwan (ICCE-TW).
- [2] Aung A T and et.al., "Influences of network delay on cooperative work in networked virtual environment with haptics," in Proc. IEEE Region 10 Conference (TENCON), pp. 1266-1271, Nov. 2020.
- [3] <https://www.3dsystems.com/haptics-devices/touch>.
- [4] <http://geomagic.com/en/products/phantom-desktop/overview>.
- [5] <http://geomagic.com/en/products/phantom-premium/overview>.
- [6] <http://www.forcedimension.com>.

- [7] [http://en.m.wikipedia.org/wiki/Haptic\\_technology](http://en.m.wikipedia.org/wiki/Haptic_technology).
- [8] Hameedha N, Ishibashi Y, and Psannis K E, "Effects of QoS control in remote master-slave robot systems with force feedback," International Journal of Mechanical Engineering and Robotics Research (IJMERR), vol. 10, no. 2, pp. 49-53, Feb. 2021.
- [9] Huang P and Ishibashi Y, "QoS control and QoE assessment in multi-sensory communications with haptics," IEICE Trans. Commun., vol. E96-B, no. 2, pp. 392-403, Feb. 2013.
- [10] Huang P and Ishibashi Y, "QoS control in remote robot operation with force feedback," IntechOpen, Robotics Software Design and Engineering, Book Chapter, pp. 1-13, Apr. 2021.
- [11] Huang P, Miyoshi T, and Ishibashi Y, "Stability control in remote bilateral robot control system with force feedback," in Proc. IEEE International Conference on Control, Automation and Robotics (ICCAR), Apr. 2017.
- [12] Ishibashi Y and Huang P, "Haptic devices," IEICE Knowledge Base, 8-1-1-1-2, pp. 5-8, May 2019.
- [13] Ishikawa S and et. al., "Effect of Robot Position Control with Force Information for Cooperative Work between Remote Robot Systems," in Proc. The 2nd World Symposium on Communication Engineering (WSCE), pp. 210-214, Dec. 2019.
- [14] Ishikawa S and et.al., "Influences of network delay on cooperative work between remote robots with force feedback," in Proc. 2020 IEEE International Conference on Computer and Communications (ICCC), pp. 548-552, Dec. 2020.
- [15] ITU E. 800, "Terms and definitions related to quality of service and network performance including dependability," Aug. 1994.
- [16] Komastu Y, Ohnashi H and Ishibashi Y, "Adaptive Control of Viscosity in Remote Control System with Force Feedback", in Proc. 2017 IEEE International Conference on Consumer Electronics - Taiwan (ICCE-TW).
- [17] Ma J and et. al., "QoE assessment of angle perception with haptics for networked virtual environments," in Proc. The 2nd International Conference on Electronics, Communications and Information Technology (CECIT), pp. 867-872, Dec. 2021.
- [18] McLaughlin M L and et.al., "The haptic Museum," in Proc. Conference on Electronic Imaging and the Visual Arts (EVA), 2000.
- [19] Novint Technologies, Inc., "Haptic device abstraction layer programmer's guide," version 1.1.9 Beta, Sep. 2007.
- [20] Ohnishi K, Katsura S and Shimono T, "Motion control for realworld haptics," IEEE Transaction on Industrial Electronics Magazine, vol. 4, no. 2, pp. 16-19, June 2010.
- [21] Oo MZ, Ishibashi Y, and Mya KT, "Influence of local lag on human perception of softness in networked virtual environment with haptic sense," ITE Trans. on Media Technology and Applications (MTA), vol. 10, no. 1, pp. 18-25, Jan. 2022.
- [22] Oo MZ, Ishibashi Y, and Mya KT, "Influences of network delay and moving velocity on virtual cooperative work with haptic sense," in Proc. The 12th International Conference on Future Computer and Communication (ICFCC), pp. 108-113, Feb. 2020.
- [23] SensAble Technologies, Inc., "openhaptics toolkit programmer's guide," version 3.4.0, 2015.
- [24] Taguchi E and et. al., "Comparison of stabilization control in cooperation between remote robots systems with force feedback," in Proc. 11th International Conference on Future Computer and Communication (ICFCC), Feb. 2019.
- [25] Wang X and et. al., "Influence of network delay on QoS control using neural network in remote robot systems with force feedback," in Proc. 2020 The 9th International Conference on Networks, Communication and Computing (ICNCC), pp. 104-111, Dec. 2020.
- [26] Wen L and et. al., "Effect of Stabilization Control by Viscosity in Remote Control System with Haptics", Japan Electronics and Information Technology Society Tokai Branch Joint Conference (9th-10th September 2019 at Daido University).
- [27] Win KZ, Ishibashi Y, and Mya KT, "QoE Assessment of Cooperative Work in Networked Virtual Environment with Haptics", Proceeding in 2021 IEEE International Conference on Consumer Electronics - Taiwan (ICCE-TW) - Special Session on Computer Communications and Signal Processing for IoT, Sep. 2021.
- [28] Win KZ, Ishibashi Y, and Win KH, "Influence of local lag on reaction force in networked virtual environment with haptic sense," in Proc. The IEEE 21st International Conference on Computer Applications (ICCA), pp. 243-247, Mar. 2024.
- [29] Win KZ, Ishibashi Y, and Win KH, "QoE Assessment of Cooperative Work in Networked Virtual Reality Environment with Haptic Sense: Influence of Network Latency," in Proc. The 5th International Conference of Advances in Information Communication Technology and Computing, AICTC 2024, April 29-30.

## Authors Profile



**Khaing Zar Win**, she got the B.C.Sc., B.C.Sc.(Hons;) and M.C.Sc. degrees in 2003, 2004 and 2009 from the University of Computer Studies, Monywa and University of Computer Studies, Mandalay respectively. She is one of the Ph.D. (IT) candidate of the University of Computer Studies, Yangon, Myanmar. She serves as a Lecturer from the University of Technology (Yatanarpon Cyber City) and as an attached Instructor at the University of Computer Studies, Yangon, Myanmar. She interests in Multimedia, Multimodal Communication, QoS Control and QoE assessment in networked haptic communication, Artificial Intelligence, Data Science.



**Yutaka Ishibashi**, he holds Ph.D. (Engineering) degree in September 1990, Nagoya Institute of Technology and serves as Professor and Dean of Faculty of Business Administration, Aichi Sangyo University, Japan. His academic activities are ACM NetGames 2006, 2010, 2013, 2017 General Co-Chair, Chairman of IEICE International Communications Quality and Reliability (CQR) Workshop 2010, 2011 Technical Program Chair, IEEE Nagoya Section Secretary (January 2015 - December 2016), IEEE Nagoya Section Chair (January 2017 - December 2018), IEEE ICCE-TW (International Conference on Consumer Electronics - Taiwan) 2018 TPC Co-Chair, ICCC (International Conference on Computer and Communications) 2018 - 2023 Conference General Chair, ICCCI (International Conference on Computer Communication and the Internet) 2020-2023 Conference Chair, Tokai Branch Chair, Institute of Image Information and Television Engineers (May 2020-April 2021), Vice-President of Institute of Image Information and Television Engineers (May 2020-May 2022), WSCE (World Symposium on Communication Engineering) 2021, 2022, 2023 Conference Chair, Information Processing Society of Japan, Tokai Branch Chair (April



2022 to May 2023), IEEE LMAG Nagoya Secretary (2024) From January). He interests in multisensory communication quality, communication quality control, haptic communication, force feedback, remote robot control.

**Amy Tun**, she holds the Ph.D. (IT) degree from the University of Computer Studies, Yangon, Myanmar. She serves as a Professor at the Faculty of Computer Systems and Technologies, University of Computer Studies, Yangon, Myanmar. She interests in IoT, Embedded Systems, Digital Image Processing, QoS Control and QoE assessment in networked haptic communication.



**Khaing Htet Win**, she holds the Ph.D. (IT) degree in 2016 from the University of Computer Studies, Yangon, Myanmar. She serves as an Associate Professor at the University of Computer Studies, PaThein, Myanmar. She interests in Natural Language Processing, Artificial Intelligence, IoT, Fuzzy Logic System, QoS Control and QoE assessment in networked haptic communication.